# A modified Darcy's law for viscoelastic flows of highly dilute polymer solutions through porous media

Omar Mokhtari, Jean-Claude Latché, Michel Quintard, Yohan Davit

# A modified Darcy's law for viscoelastic flows of highly dilute polymer solutions through porous media

Omar Mokhtari[1,2], Jean-Claude Latché[3], Michel Quintard[1], Yohan Davit[1,†]

[1] *Institut de Mécanique des fluides de Toulouse (IMFT), CNRS & Université de Toulouse, France*
[2] *TotalEnergies E&P, CSTJF, Pau, France*
[3] *Institut de Radioprotection et de Sûreté Nucléaire (IRSN), France*

**Abstract**

Viscoelastic flows of polymer solutions in complex geometries can generate a strong localization of stress within small regions of the fluid and the formation of birefringent strands. In porous media, these localized structures of stress drive preferential flow paths and increase global dissipation. Modeling the impact of such effects at Darcy or larger scales is a daunting task – one of the reasons being the lack of approaches using homogenization theories to help figure out both the correct form of the averaged transport equations and the relevant set of effective parameters. Here we homogenize the incompressible Oldroyd-B equations at zero Reynolds number to obtain a Darcy scale model that captures the effect of localized polymeric stress. This model consists of an advection-reaction transport equation for the average conformation tensor along with a form of Darcy's law that contains an additional drag term associated with structures of localized stress. The derivation is based upon a limit of high dilution, a regime where the Oldroyd-B model can be transformed into a sequence of linear problems using asymptotic developments. We validate our approach in test cases corresponding to flows in a channel and through arrays of circles. Besides providing a new model for viscoelastic flows in porous media, our work also shows that modelling viscoelastic flows through porous media is not simply a matter of determining an apparent permeability tensor – the homogenized model cannot be easily reduced to a simple form of Darcy's law – but rather requires the development of specific homogenized models that capture the coupling between the transport of the polymeric stress and momentum.

## 1. Introduction

Modeling the flow of viscoelastic polymer solutions through porous media is a problem of interest in a number of engineering applications including soil remediation processes or enhanced oil recovery [12, 29, 44, 46, 47]. Solving viscoelastic flows at pore-scale in complex structures is challenging, even for moderate Weissenberg numbers – the dimensionless number that measures the relative importance of elastic effects. This issue is often referred to as

*Email address:* yohan.davit@imft.fr (Yohan Davit[1,†])

the High Weissenberg Number Problem (HWNP) [6, 7, 25, 27, 39] and stems from a strong localization of the polymeric stress in small regions of the domain where the conformation tensor can reach extremely high values. The archetypal example is the birefringent strand observed past a single cylinder [18, 22, 49] or in cross-slot devices [33, 37, 43]. This HWNP strongly constrains the simulations with strong limits upon accessible Weissenberg numbers and upon the extent of the simulation domains [28, 53]. Deriving average formulations that do not require the detailed description at pore-scale, but rather capture small-scale phenomena through effective parameters at larger scale, is an interesting fundamental problem and would also be a useful tool in engineering applications.

A few computations of apparent permeabilities are available in the literature [2, 10, 20, 31, 48, 50]. However, there are very few works attempting to perform a direct homogenization of viscoelastic flows through porous media and, in so doing, to question the form of the macroscale equations and the relevant set of effective parameters. Khuzhayorov et al. [30] used formal multiple scale asymptotics and De Haro et al. [11] used volume averaging to derive a form of dynamic Darcy's law. Unfortunately, the homogenization in both these works is limited to a linear form of viscoelasticity with a constitutive equation that is not frame indifferent and that does not capture transport of the polymeric stress – it is similar to a low Weissenberg approximation. This approach eliminates right away terms that actually generate the birefringent strands, in particular an important part of the upper-convected derivative in the transport of the conformation tensor. Slattery [45] proposes a generalization of the resistance tensor for several fluids, including a Noll simple fluid, but without performing the homogenization of the constitutive equation.

In this work, we use volume averaging to derive a homogenized model starting from the incompressible Oldroyd-B equations at low Reynolds number [3, 38],

$$0 = -\nabla p + \Delta \mathbf{u} + \frac{\beta}{Wi} \nabla \cdot \mathbf{C} + \mathbf{F}, \tag{1.1a}$$

$$0 = \nabla \cdot \mathbf{u}, \tag{1.1b}$$

$$\partial_t \mathbf{C} + \mathbf{u} \cdot \nabla \mathbf{C} = \nabla \mathbf{u} \cdot \mathbf{C} + \mathbf{C} \cdot \nabla \mathbf{u}^{\mathsf{T}} - \frac{1}{Wi} \left( \mathbf{C} - \mathbf{I}_d \right), \tag{1.1c}$$

with a no-slip and no-penetration boundary condition for fluid/solid interfaces. Here $p$ is a dimensionless pressure, $\mathbf{u}$ a dimensionless velocity, $\mathbf{C}$ the conformation tensor, $\mathbf{I}_d$ the identity in dimension $d = 2$ or 3 and $\mathbf{F}$ a constant/uniform dimensionless force density vector field. $\beta \overset{\text{def}}{=} \eta_p/\eta_s$ is the ratio of polymeric to solvent viscosities and $Wi \overset{\text{def}}{=} \lambda U/H$ is the Weissenberg number with $\lambda$ the relaxation time of the polymer, $U$ a reference velocity and $H$ a characteristic lengthscale.

Our idea is to perform the homogenization in a limit that allows us to derive a linearized form of the problem but that still captures the stress localization. $Wi \ll 1$ is frequently used for the linearization but does not capture the stress localization that appears for moderate Weissenberg numbers. Instead, we proceed by considering the limit $\beta \ll 1$ that can be thought of as a limit of large dilution for polymer solutions ($\eta_p$ small and thus $\beta$ small). In this case, the leading order for the velocity is simply the Newtonian field with viscosity $\eta_s$ and the leading order for the conformation tensor corresponds to the transport in Eq 1.1c

with the Newtonian velocity, therefore transforming the problem into a sequence of linear problems with one-way couplings. This makes it possible to treat cases with relatively large $Wi$ numbers and thus to derive a form of Darcy's law that captures some of the fundamental features of viscoelastic flows, such as birefringent strands.

The paper is organized as follows. In Section 2, we detail the non-dimensionalization of the problem, reformulate the Oldroyd-B model in terms of a conformation vector, rather than a matrix, and derive the sequence of problems in the limit $\beta \ll 1$. We then proceed in Section 3 to averaging the partial differential equations at each order in the asymptotic developments and to deriving the corresponding average model. To finish, we study in Section 4 the behaviour of our model for three 2D test cases in simple geometries (channel, crystalline and amorphous periodic structures of circles).

## 2. Reformulation of the flow problem

### *2.1. Non-dimensionalization*

In the Introduction, Eq 1.1 is a dimensionless form of the Oldroyd-B problem. Here we show how to obtain this form starting from the dimensional form of the Oldroyd-B problem

$$0 = -\nabla \mathfrak{p} + \eta_s \Delta \mathfrak{u} + \frac{\eta_p}{\lambda} \nabla \cdot \mathbf{C} + \mathfrak{F}, \tag{2.1a}$$

$$0 = \nabla \cdot \mathfrak{u}, \tag{2.1b}$$

$$\partial_t \mathbf{C} + \mathfrak{u} \cdot \nabla \mathbf{C} = \nabla \mathfrak{u} \cdot \mathbf{C} + \mathbf{C} \cdot \nabla \mathfrak{u}^{\mathsf{T}} - \frac{1}{\lambda} \left( \mathbf{C} - \mathbf{I}_d \right). \tag{2.1c}$$

$\mathfrak{u}$ and $\mathfrak{p}$ are the velocity and pressure, respectively. $\mathfrak{F}$ is the dimensional force density vector field that we take constant and uniform. $\eta_s$ and $\eta_p$ are solvent and polymeric viscosities, respectively. $\lambda$ is a characteristic time associated with the relaxation of the polymers. This problem may be written in dimensionless form as

$$0 = -\nabla p + \Delta \mathbf{u} + \frac{\beta}{Wi} \nabla \cdot \mathbf{C} + \mathbf{F}, \tag{2.2a}$$

$$0 = \nabla \cdot \mathbf{u}, \tag{2.2b}$$

$$\partial_t \mathbf{C} + \mathbf{u} \cdot \nabla \mathbf{C} = \nabla \mathbf{u} \cdot \mathbf{C} + \mathbf{C} \cdot \nabla \mathbf{u}^{\mathsf{T}} - \frac{1}{Wi} \left( \mathbf{C} - \mathbf{I}_d \right), \tag{2.2c}$$

with

$$\mathbf{x} \stackrel{\text{def}}{=} \frac{\mathfrak{x}}{H}, \quad t \stackrel{\text{def}}{=} \frac{\|\mathfrak{F}\| H}{\eta_s} \mathfrak{t}, \quad p \stackrel{\text{def}}{=} \frac{\mathfrak{p}}{\|\mathfrak{F}\| H}, \quad \mathbf{F} \stackrel{\text{def}}{=} \frac{\mathfrak{F}}{\|\mathfrak{F}\|}, \quad \beta \stackrel{\text{def}}{=} \frac{\eta_p}{\eta_s}, \quad Wi \stackrel{\text{def}}{=} \frac{\lambda \|\mathfrak{F}\| H}{\eta_s}.$$

### *2.2. Vector form of the transport equations*

The transport equation for the conformation tensor in the fluid domain $\Omega_f$ is

$$\partial_t \mathbf{C} + \mathbf{u} \cdot \nabla \mathbf{C} = \nabla \mathbf{u} \cdot \mathbf{C} + \mathbf{C} \cdot \nabla \mathbf{u}^{\mathsf{T}} - \frac{1}{Wi} \left( \mathbf{C} - \mathbf{I}_d \right), \tag{2.3}$$

with $\mathbf{C}(\mathbf{x},t) \in \mathbb{R}^{d\times d}_{S,>0}$ a symmetric ($S$) positive ($>0$) $d\times d$ matrix with $d=2$ or 3. Dealing with the transport of a matrix in the homogenization procedure is tedious. Closure relationships for $\mathbf{C}$ would involve tensors of at least rank 4, with complex symmetries and the process would be extremely cumbersome. The homogenization procedure can be greatly simplified with a reformulation of the problem in terms of a vector, $\mathbf{c}(\mathbf{x},t) \in \mathbb{R}^{\frac{d(d+1)}{2}}$, defined such that $\mathbf{c} \overset{\text{def}}{=} \begin{pmatrix} C_{xx} & C_{yy} & C_{xy} \end{pmatrix}^\mathsf{T}$ in 2D and $\mathbf{c} \overset{\text{def}}{=} \begin{pmatrix} C_{xx} & C_{yy} & C_{zz} & C_{yz} & C_{xz} & C_{xy} \end{pmatrix}^\mathsf{T}$ in 3D. This approach is reminiscent of the Voigt and Mandel notation often used in linear elasticity [13, 24, 32, 52]. The new transport equation can be written as

$$\partial_t \mathbf{c} + \mathbf{u}\cdot\nabla\mathbf{c} = (D\mathbf{u})\cdot\mathbf{c} - \frac{1}{Wi}(\mathbf{c}-\mathbf{i}) \tag{2.4}$$

with

$$D\mathbf{u} \overset{\text{def}}{=} \begin{pmatrix} 2\partial_x u_x & 0 & 2\partial_y u_x \\ 0 & 2\partial_y u_y & 2\partial_x u_y \\ \partial_x u_y & \partial_y u_x & 0 \end{pmatrix} \text{ for } d=2, \tag{2.5}$$

and

$$D\mathbf{u} \overset{\text{def}}{=} \begin{pmatrix} 2\partial_x u_x & 0 & 0 & 0 & 2\partial_z u_x & 2\partial_y u_x \\ 0 & 2\partial_y u_y & 0 & 2\partial_z u_y & 0 & 2\partial_x u_y \\ 0 & 0 & 2\partial_z u_z & 2\partial_y u_z & 2\partial_x u_z & 0 \\ 0 & \partial_y u_z & \partial_z u_y & \partial_y u_y + \partial_z u_z & \partial_x u_y & \partial_x u_z \\ \partial_x u_y & \partial_y u_x & 0 & \partial_z u_x & \partial_z u_y & \partial_x u_x + \partial_y u_y \\ \partial_x u_z & 0 & \partial_z u_x & \partial_y u_x & \partial_x u_x + \partial_z u_z & \partial_y u_z \end{pmatrix} \text{ for } d=3, \tag{2.6}$$

and

$$\mathbf{i} \overset{\text{def}}{=} \begin{pmatrix} 1 \\ 1 \\ 0 \end{pmatrix} \text{ for } d=2 \text{ and } \mathbf{i} \overset{\text{def}}{=} \begin{pmatrix} 1 \\ 1 \\ 1 \\ 0 \\ 0 \\ 0 \end{pmatrix} \text{ for } d=3. \tag{2.7}$$

Note in particular that $D\mathbf{u}\cdot\mathbf{i} = \nabla\mathbf{u} + (\nabla\mathbf{u})^\mathsf{T}$.

For the momentum transport equation, we rewrite this as

$$0 = -\nabla p + \Delta\mathbf{u} + \frac{\beta}{Wi}\nabla_c\cdot\boldsymbol{c} \tag{2.8}$$

with

$$\nabla_c \overset{\text{def}}{=} \begin{pmatrix} \partial_x & 0 & \partial_y \\ 0 & \partial_y & \partial_x \end{pmatrix} \text{ for } d=2 \text{ and } \nabla_c \overset{\text{def}}{=} \begin{pmatrix} \partial_x & 0 & 0 & 0 & \partial_z & \partial_y \\ 0 & \partial_y & 0 & \partial_z & 0 & \partial_x \\ 0 & 0 & \partial_z & \partial_y & \partial_x & 0 \end{pmatrix} \text{ for } d=3. \tag{2.9}$$

Note in particular that $(\nabla_c\cdot D\mathbf{u})\cdot\mathbf{i} = \Delta\mathbf{u}$.

The final form of the system of equations is thus

$$0 = -\nabla p + \Delta \mathbf{u} + \frac{\beta}{Wi} \nabla_c \cdot \boldsymbol{c} + \mathbf{F}, \tag{2.10a}$$

$$0 = \nabla \cdot \mathbf{u}, \tag{2.10b}$$

$$\partial_t \mathbf{c} + \mathbf{u} \cdot \nabla \mathbf{c} = (D\mathbf{u})\,\mathbf{c} - \frac{1}{Wi}\left(\mathbf{c} - \mathbf{i}\right). \tag{2.10c}$$

*2.3. Approximate form of transport through $\beta$ asymptotics*

To perform the asymptotic development, we use the standard mathematical approach [21, 19, 51] that consists in scaling the dimensionless parameters as a function of a small parameter, $\varepsilon$, and searching for solutions in the form of series of $\varepsilon$. The limit $Wi = O(\varepsilon^n)$ with $n \geq 1$ is trivial (see e.g. detailed asymptotics in [4, 36]), yielding a standard Darcy's law with a viscosity $1 + \beta$ at leading-order. This case does not require considering asymptotics in $\beta$. Our interest is in the case $Wi = O(1)$ and $\beta = O(\epsilon)$ where strands start forming. Cases of large Weissenberg numbers can also be treated following a similar strategy, but the most interesting case is actually $Wi = O(1)$ because it maintains a competition between stretching and relaxation in the transport equation for the conformation tensor.

For $Wi = O(1)$ and $\beta = O(\epsilon)$, we write $\beta = \varepsilon\beta^\star$ and have

$$0 = -\nabla p + \Delta \mathbf{u} + \varepsilon\frac{\beta^\star}{Wi} \nabla_c \cdot \boldsymbol{c} + \mathbf{F}, \tag{2.11a}$$

$$0 = \nabla \cdot \mathbf{u}, \tag{2.11b}$$

$$\partial_t \mathbf{c} + \mathbf{u} \cdot \nabla \mathbf{c} = (D\mathbf{u})\,\mathbf{c} - \frac{1}{Wi}\left(\mathbf{c} - \mathbf{i}\right). \tag{2.11c}$$

. We are looking for a solution in the form

$$p = p^{(0)} + \varepsilon p^{(1)}, \tag{2.12a}$$

$$\mathbf{u} = \mathbf{u}^{(0)} + \varepsilon \mathbf{u}^{(1)}, \tag{2.12b}$$

$$\mathbf{c} = \mathbf{c}^{(0)}, \tag{2.12c}$$

in order to obtain a sequence of problem corresponding to the different orders. At leading order for the momentum transport and mass conservation, we have

$$0 = -\nabla p^{(0)} + \Delta \mathbf{u}^{(0)} + \mathbf{F}, \tag{2.13a}$$

$$0 = \nabla \cdot \mathbf{u}^{(0)}, \tag{2.13b}$$

and for the transport of the conformation tensor

$$\partial_t \mathbf{c}^{(0)} + \mathbf{u}^{(0)} \cdot \nabla \mathbf{c}^{(0)} = D\mathbf{u}^{(0)}\mathbf{c}^{(0)} - \frac{1}{Wi}\left(\mathbf{c}^{(0)} - \mathbf{i}\right). \tag{2.14}$$

At first order for momentum and mass conservation, we have

$$0 = -\nabla p^{(1)} + \Delta \mathbf{u}^{(1)} + \frac{\beta^\star}{Wi} \nabla_c \cdot \mathbf{c}^{(0)}, \tag{2.15a}$$

$$0 = \nabla \cdot \mathbf{u}^{(1)}. \tag{2.15b}$$

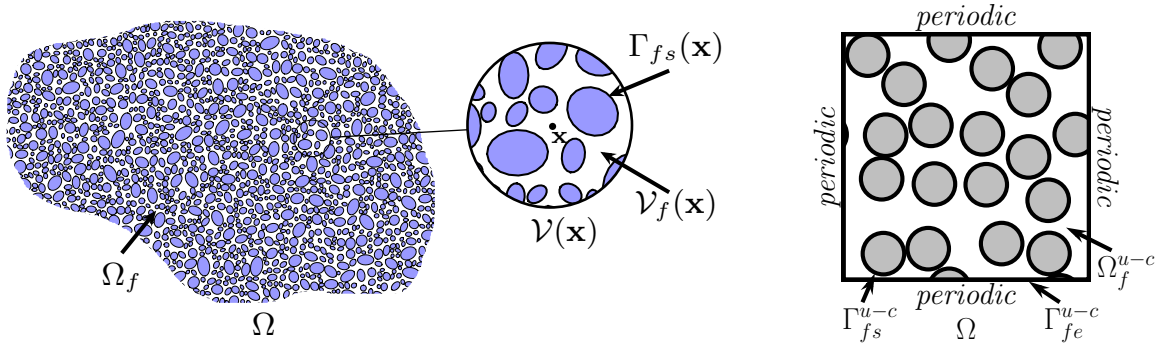


(a) Large scale domain and averaging volume (b) Unit-cell

Figure 3.1: Schematics of the volume averaging procedure with (a) the large scale domain, magnifications for the averaging volume at point $\mathbf{x}$ and notations for the sets considered; and (b) a unit-cell with corresponding notations.

## 3. Homogenization through volume averaging

### *3.1. Definitions*

We define the intrinsic average operator as

$$\langle \chi \rangle (\mathbf{x}) = \frac{\int_{\mathcal{V}_f(\mathbf{x})} \chi \, dV}{\int_{\mathcal{V}_f(\mathbf{x})} dV}. \tag{3.1}$$

The porosity $\phi$ is

$$\phi = \frac{\int_{\mathcal{V}_f(\mathbf{x})} dV}{\int_{\mathcal{V}(\mathbf{x})} dV}. \tag{3.2}$$

To simplify the developments, we also consider a porous structure such that $\int_{\mathcal{V}_f} dV$ and the porosity are uniform and constant. Important notations for the averaging procedure are summarized in Fig 3.1.

Note that in this paper, $\langle \chi \rangle$ refers to the intrinsic average of $\chi$, which is not the most standard notation in the volume averaging literature (usually we use $\langle \rangle^{\text{fluid}}$ or similar) but is more compact and simpler when the porosity is constant and uniform.

### *3.2. Volume averaging for the transport of* $\mathbf{u}^{(0)}$

We indicate key steps here as the technique is described in details in many works (see for instance [55, 54, 9]). First, we average

$$0 = -\nabla p^{(0)} + \Delta \mathbf{u}^{(0)} + \mathbf{F}, \qquad \text{in } \Omega_f \tag{3.3a}$$

$$0 = \nabla \cdot \mathbf{u}^{(0)}, \qquad \text{in } \Omega_f \tag{3.3b}$$

$$\mathbf{u}^{(0)} = 0, \qquad \text{on } \Gamma_{fs} \tag{3.3c}$$

considering a no-slip/no-penetration boundary condition on the fluid/solid interface $\Gamma_{fs}$. We then use the average plus perturbation decomposition

$$p^{(0)} = \left\langle p^{(0)} \right\rangle + \tilde{p}^{(0)}, \tag{3.4a}$$

$$\mathbf{u}^{(0)} = \left\langle \mathbf{u}^{(0)} \right\rangle + \tilde{\mathbf{u}}^{(0)}, \tag{3.4b}$$

to obtain

$$0 = -\nabla \left\langle p^{(0)} \right\rangle + \left\langle -\nabla \tilde{p}^{(0)} + \Delta \tilde{\mathbf{u}}^{(0)} \right\rangle + \mathbf{F}, \tag{3.5a}$$

$$0 = \nabla \cdot \left\langle \mathbf{u}^{(0)} \right\rangle, \tag{3.5b}$$

where the Brinkman term $\Delta \left\langle \mathbf{u}^{(0)} \right\rangle$ has been removed as is standard Whitaker [55]. The perturbation equation reads

$$0 = -\nabla \tilde{p}^{(0)} + \Delta \tilde{\mathbf{u}}^{(0)} - \left\langle -\nabla \tilde{p}^{(0)} + \Delta \tilde{\mathbf{u}}^{(0)} \right\rangle \quad \text{in } \Omega_f \tag{3.6a}$$

$$0 = \nabla \cdot \tilde{\mathbf{u}}^{(0)} \quad \text{in } \Omega_f \tag{3.6b}$$

$$\tilde{\mathbf{u}}^{(0)} = -\left\langle \mathbf{u}^{(0)} \right\rangle \quad \text{on } \Gamma_{fs} \tag{3.6c}$$

and is simply obtained by subtracting Eqs 3.5a and 3.5b from Eqs 3.3a and 3.3b, respectively. Because of the linearity of the problem, we may seek a solution of the problem in the form

$$\tilde{p}^{(0)} = -\mathbf{b}^{(0)} \cdot \left\langle \mathbf{u}^{(0)} \right\rangle, \tag{3.7a}$$

$$\tilde{\mathbf{u}}^{(0)} = -\mathbf{B}^{(0)} \cdot \left\langle \mathbf{u}^{(0)} \right\rangle, \tag{3.7b}$$

with the corresponding closure problem

$$0 = -\nabla \mathbf{b}^{(0)} + \Delta \mathbf{B}^{(0)} - \left\langle -\nabla \mathbf{b}^{(0)} + \Delta \mathbf{B}^{(0)} \right\rangle \quad \text{in } \Omega_f^{\text{u-c}} \tag{3.8a}$$

$$0 = \nabla \cdot \mathbf{B}^{(0)} \quad \text{in } \Omega_f^{\text{u-c}} \tag{3.8b}$$

$$\mathbf{B}^{(0)} = \mathbf{I}_d \quad \text{on } \Gamma_{fs}^{\text{u-c}} \tag{3.8c}$$

$$\text{Periodicity} \quad \text{on } \Gamma_{fe}^{\text{u-c}} \tag{3.8d}$$

$$\text{Averages } \left\langle \mathbf{b}^{(0)} \right\rangle = 0 \text{ and } \left\langle \mathbf{B}^{(0)} \right\rangle = 0 \tag{3.8e}$$

This problem is used to calculate the effective parameters appearing in the macroscale equations. The periodicity on boundary conditions for the outside of the unit-cell ($\Gamma_{fe}^{\text{u-c}}$) is the standard approach [42, 54].

The macroscale equation is obtained by introducing the closure relations into Eq 3.5a to obtain

$$0 = -\nabla \left\langle p^{(0)} \right\rangle - \left\langle -\nabla \mathbf{b}^{(0)} + \Delta \mathbf{B}^{(0)} \right\rangle \cdot \left\langle \mathbf{u}^{(0)} \right\rangle, \tag{3.9a}$$

$$0 = \nabla \cdot \left\langle \mathbf{u}^{(0)} \right\rangle. \tag{3.9b}$$

We further define the Darcy velocity

$$\left\langle \mathbf{u}^{(0)} \right\rangle^D \stackrel{\text{def}}{=} \phi \left\langle \mathbf{u}^{(0)} \right\rangle \tag{3.10}$$

and

$$\mathbf{K}^{-1} \overset{\text{def}}{=} \phi^{-1} \left\langle -\nabla \mathbf{b}^{(0)} + \Delta \mathbf{B}^{(0)} \right\rangle, \tag{3.11}$$

assuming that $\mathbf{K}$ is invertible. We then obtain Darcy's law

$$\left\langle \mathbf{u}^{(0)} \right\rangle^{D} = \mathbf{K} \cdot \left( -\nabla \left\langle p^{(0)} \right\rangle + \mathbf{F} \right). \tag{3.12}$$

Note that we can reformulate the problem for $\mathbf{b}^{(0)}$ and $\mathbf{B}^{(0)}$ using the change of unknown functions

$$\mathbf{b}^{(0)} = \mathbf{g} \cdot \phi \mathbf{K}^{-1} \tag{3.13}$$

$$\mathbf{B}^{(0)} = \mathbf{I}_d + \mathbf{G} \cdot \phi \mathbf{K}^{-1} \tag{3.14}$$

with

$$0 = -\nabla \mathbf{g} + \Delta \mathbf{G} - \mathbf{I}_d \qquad \text{in } \Omega_f^{\text{u-c}} \tag{3.15a}$$

$$0 = \nabla \cdot \mathbf{G} \qquad \text{in } \Omega_f^{\text{u-c}} \tag{3.15b}$$

$$\mathbf{G} = 0 \qquad \text{on } \Gamma_{fs}^{\text{u-c}} \tag{3.15c}$$

$$\text{Periodicity} \qquad \text{on } \Gamma_{fe}^{\text{u-c}} \tag{3.15d}$$

$$\text{Average } \langle \mathbf{g} \rangle = 0 \tag{3.15e}$$

$\left\langle \mathbf{b}^{(0)} \right\rangle = 0$ implies that $\langle \mathbf{g} \rangle = 0$ and $\left\langle \mathbf{B}^{(0)} \right\rangle = 0$ leads to $\mathbf{I}_d + \langle \mathbf{G} \rangle \cdot \phi \mathbf{K}^{-1} = 0$ and thus

$$\mathbf{K} = -\phi \langle \mathbf{G} \rangle. \tag{3.16}$$

The advantage of solving the problem for $(\mathbf{g},\ \mathbf{G})$ rather than the one for $\left(\mathbf{b}^{(0)},\ \mathbf{B}^{(0)}\right)$ is that it is differential and not integro-differential.

### *3.3. Volume averaging for the transport of the conformation tensor*

We now proceed to averaging the transport equation for the conformation tensor at leading order

$$\partial_t \mathbf{c}^{(0)} + \mathbf{u}^{(0)} \cdot \nabla \mathbf{c}^{(0)} = D\mathbf{u}^{(0)} \mathbf{c}^{(0)} - \frac{1}{Wi} \left( \mathbf{c}^{(0)} - \mathbf{i} \right). \tag{3.17}$$

We use the average plus perturbation decomposition

$$\mathbf{c}^{(0)} = \left\langle \mathbf{c}^{(0)} \right\rangle + \widetilde{\mathbf{c}}^{(0)} \tag{3.18}$$

We have $\left\langle \partial_t \mathbf{c}^{(0)} \right\rangle = \partial_t \left\langle \mathbf{c}^{(0)} \right\rangle$ since there is no time variation of the geometry. We also have

$$\left\langle \mathbf{u}^{(0)} \cdot \nabla \mathbf{c}^{(0)} \right\rangle = \left\langle \mathbf{u}^{(0)} \right\rangle \cdot \nabla \left\langle \mathbf{c}^{(0)} \right\rangle + \left\langle \mathbf{u}^{(0)} \cdot \nabla \widetilde{\mathbf{c}}^{(0)} \right\rangle, \tag{3.19}$$

$$\left\langle D\mathbf{u}^{(0)} \cdot \mathbf{c}^{(0)} \right\rangle^{f} = \left\langle D\mathbf{u}^{(0)} \right\rangle \cdot \left\langle \mathbf{c}^{(0)} \right\rangle + \left\langle D\mathbf{u}^{(0)} \cdot \widetilde{\mathbf{c}}^{(0)} \right\rangle. \tag{3.20}$$

Averaging thus leads to

$$\partial_t \left\langle \mathbf{c}^{(0)} \right\rangle + \left\langle \mathbf{u}^{(0)} \right\rangle \cdot \nabla \left\langle \mathbf{c}^{(0)} \right\rangle = \left\langle D\mathbf{u}^{(0)} \right\rangle \cdot \left\langle \mathbf{c}^{(0)} \right\rangle - \frac{1}{Wi} \left( \left\langle \mathbf{c}^{(0)} \right\rangle - \mathbf{i} \right) - \left\langle \mathbf{u}^{(0)} \cdot \nabla \widetilde{\mathbf{c}}^{(0)} \right\rangle + \left\langle D\mathbf{u}^{(0)} \cdot \widetilde{\mathbf{c}}^{(0)} \right\rangle \tag{3.21}$$

Upon neglecting terms in $\nabla \left\langle \mathbf{c}^{(0)} \right\rangle$ (leading order in $\left\langle \mathbf{c}^{(0)} \right\rangle$) and assuming quasi-stationarity, the perturbation equation reads

$$\mathbf{u}^{(0)} \cdot \nabla \widetilde{\mathbf{c}}^{(0)} - \left\langle \mathbf{u}^{(0)} \cdot \nabla \widetilde{\mathbf{c}}^{(0)} \right\rangle = \left( D\mathbf{u}^{(0)} \cdot \widetilde{\mathbf{c}}^{(0)} - \left\langle D\mathbf{u}^{(0)} \cdot \widetilde{\mathbf{c}}^{(0)} \right\rangle \right) - \frac{1}{Wi} \widetilde{\mathbf{c}}^{(0)} + \widetilde{D}\mathbf{u}^{(0)} \cdot \left\langle \mathbf{c}^{(0)} \right\rangle, \tag{3.22}$$

which is obtained by subtracting Eq 3.21 from Eq 3.17. Because of the linearity, we write a closure in the form

$$\widetilde{\mathbf{c}}^{(0)} = \mathbf{A} \cdot \left\langle \mathbf{c}^{(0)} \right\rangle, \tag{3.23}$$

so that

$$\mathbf{u}^{(0)} \cdot \nabla \mathbf{A} = D\mathbf{u}^{(0)} \cdot \mathbf{A} - \frac{1}{We} \mathbf{A} + D\mathbf{u}^{(0)} - \mathbf{B} \qquad \text{in } \Omega_f^{\text{u-c}} \tag{3.24a}$$

$$\text{with } \langle \mathbf{A} \rangle = 0, \tag{3.24b}$$

$$\text{and } \mathbf{B} = \left\langle D\mathbf{u}^{(0)} \cdot \left( \mathbf{I}_{\frac{d(d+1)}{2}} + \mathbf{A} \right) \right\rangle - \left\langle \mathbf{u}^{(0)} \cdot \nabla \mathbf{A} \right\rangle, \tag{3.24c}$$

$$\text{and periodicity} \qquad \text{on } \Gamma_{fe}^{\text{u-c}} \tag{3.24d}$$

Again this equation is integro-differential but can be simplified through the decomposition

$$\mathbf{A} = \left( \mathbf{M} - \mathbf{I}_{\frac{d(d+1)}{2}} \right) - Wi \; \mathbf{M} \cdot \mathbf{B} \tag{3.25}$$

with $\mathbf{M}$ solution of

$$\mathbf{u}^{(0)} \cdot \nabla \mathbf{M} = D\mathbf{u}^{(0)} \cdot \mathbf{M} - \frac{1}{Wi} \left( \mathbf{M} - \mathbf{I}_{\frac{d(d+1)}{2}} \right) \qquad \text{in } \Omega_f^{\text{u-c}} \tag{3.26a}$$

$$\text{Periodicity} \qquad \text{on } \Gamma_{fe}^{\text{u-c}} \tag{3.26b}$$

$\langle \mathbf{A} \rangle = 0$ implies that

$$\mathbf{B} = Wi^{-1} \left( \mathbf{I}_{\frac{d(d+1)}{2}} - \langle \mathbf{M} \rangle^{-1} \right). \tag{3.27}$$

Also note that $\mathbf{A} = \mathbf{M} \cdot \langle \mathbf{M} \rangle^{-1} - \mathbf{I}_{\frac{d(d+1)}{2}}$ so that

$$\mathbf{c}^{(0)} = \mathbf{M} \cdot \langle \mathbf{M} \rangle^{-1} \cdot \left\langle \mathbf{c}^{(0)} \right\rangle. \tag{3.28}$$

The macroscopic equation reads

$$\partial_t \left\langle \mathbf{c}^{(0)} \right\rangle + \left\langle \mathbf{u}^{(0)} \right\rangle \cdot \nabla \left\langle \mathbf{c}^{(0)} \right\rangle = \mathbf{B} \cdot \left\langle \mathbf{c}^{(0)} \right\rangle - \frac{1}{Wi} \left( \left\langle \mathbf{c}^{(0)} \right\rangle - \mathbf{i} \right). \tag{3.29}$$

*3.4. Volume averaging for the transport of* $\mathbf{u}^{(1)}$

At first order, we have

$$0 = -\nabla p^{(1)} + \Delta \mathbf{u}^{(1)} + \frac{\beta^\star}{Wi}\nabla_c \cdot \mathbf{c}^{(0)}, \qquad \text{in } \Omega_f \tag{3.30a}$$

$$0 = \nabla \cdot \mathbf{u}^{(1)}, \qquad \text{in } \Omega_f \tag{3.30b}$$

$$\mathbf{u}^{(1)} = 0 \qquad \text{on } \Gamma_{fs} \tag{3.30c}$$

that we average as

$$0 = -\nabla \left\langle p^{(1)} \right\rangle + \Delta \left\langle \mathbf{u}^{(1)} \right\rangle + \frac{\beta^\star}{Wi}\nabla_c \cdot \left\langle \mathbf{c}^{(0)} \right\rangle + \left\langle -\nabla \tilde{p}^{(1)} + \Delta \tilde{\mathbf{u}}^{(1)} + \frac{\beta^\star}{Wi}\nabla_c \cdot \widetilde{\mathbf{c}}^{(0)} \right\rangle, \tag{3.31a}$$

$$0 = \nabla \cdot \left\langle \mathbf{u}^{(1)} \right\rangle. \tag{3.31b}$$

The perturbation equation is

$$0 = -\nabla \tilde{p}^{(1)} + \Delta \tilde{\mathbf{u}}^{(1)} + \frac{\beta^\star}{Wi}\nabla_c \cdot \widetilde{\mathbf{c}}^{(0)} - \left\langle -\nabla \tilde{p}^{(1)} + \Delta \tilde{\mathbf{u}}^{(1)} + \frac{\beta^\star}{Wi}\nabla_c \cdot \widetilde{\mathbf{c}}^{(0)} \right\rangle \qquad \text{in } \Omega_f \tag{3.32a}$$

$$0 = \nabla \cdot \tilde{\mathbf{u}}^{(1)} \qquad \text{in } \Omega_f \tag{3.32b}$$

$$\tilde{\mathbf{u}}^{(1)} = -\left\langle \mathbf{u}^{(1)} \right\rangle \qquad \text{on } \Gamma_{fs} \tag{3.32c}$$

Upon using

$$\widetilde{\mathbf{c}}^{(0)} = \left( \mathbf{M} \cdot \langle \mathbf{M} \rangle^{-1} - \mathbf{I}_{\frac{d(d+1)}{2}} \right) \cdot \left\langle \mathbf{c}^{(0)} \right\rangle, \tag{3.33}$$

we have

$$\nabla_c \cdot \widetilde{\mathbf{c}}^{(0)} = \nabla_c \cdot \left( \mathbf{M} \cdot \langle \mathbf{M} \rangle^{-1} \right) \cdot \left\langle \mathbf{c}^{(0)} \right\rangle \tag{3.34}$$

so that

$$\begin{aligned} 0 = &-\nabla \tilde{p}^{(1)} + \Delta \tilde{\mathbf{u}}^{(1)} - \left\langle -\nabla \tilde{p}^{(1)} + \Delta \tilde{\mathbf{u}}^{(1)} \right\rangle \qquad \text{in } \Omega_f \\ &+ \frac{\beta^\star}{Wi}\nabla_c \cdot \left( \mathbf{M} \cdot \langle \mathbf{M} \rangle^{-1} \right) \cdot \left\langle \mathbf{c}^{(0)} \right\rangle - \frac{\beta^\star}{Wi} \left\langle \nabla_c \cdot \left( \mathbf{M} \cdot \langle \mathbf{M} \rangle^{-1} \right) \right\rangle \cdot \left\langle \mathbf{c}^{(0)} \right\rangle \end{aligned} \tag{3.35a}$$

$$0 = \nabla \cdot \tilde{\mathbf{u}}^{(1)} \qquad \text{in } \Omega_f \tag{3.35b}$$

$$\tilde{\mathbf{u}}^{(1)} = -\left\langle \mathbf{u}^{(1)} \right\rangle \qquad \text{on } \Gamma_{fs} \tag{3.35c}$$

We have the following closure

$$\tilde{p}^{(1)} = -\mathbf{b}^{(0)} \cdot \left\langle \mathbf{u}^{(1)} \right\rangle - \frac{\beta^\star}{Wi} \boldsymbol{P}^{(1)} \cdot \left\langle \mathbf{c}^{(0)} \right\rangle \tag{3.36a}$$

$$\tilde{\mathbf{u}}^{(1)} = -\mathbf{B}^{(0)} \cdot \left\langle \mathbf{u}^{(1)} \right\rangle - \frac{\beta^\star}{Wi} \mathbf{U}^{(1)} \cdot \left\langle \mathbf{c}^{(0)} \right\rangle \tag{3.36b}$$

with $\left( \boldsymbol{P}^{(1)},\ \mathbf{U}^{(1)} \right)$ solution of

$$0 = -\nabla \boldsymbol{P}^{(1)} + \Delta \mathbf{U}^{(1)} - \nabla_c \cdot \left( \mathbf{M} \cdot \langle \mathbf{M} \rangle^{-1} \right) - \mathbf{N} \qquad \text{in } \Omega_f^{\text{u-c}} \tag{3.37a}$$

$$0 = \nabla \cdot \mathbf{U}^{(1)} \qquad \text{in } \Omega_f^{\text{u-c}} \tag{3.37b}$$

$$\mathbf{U}^{(1)} = 0 \qquad \text{on } \Gamma_{fs}^{\text{u-c}} \tag{3.37c}$$

$$\text{Periodicity} \qquad \text{on } \Gamma_{fe}^{\text{u-c}} \tag{3.37d}$$

$$\text{Averages } \left\langle \boldsymbol{P}^{(1)} \right\rangle = 0 \text{ and } \left\langle \mathbf{U}^{(1)} \right\rangle = 0 \tag{3.37e}$$

with

$$\mathbf{N} \overset{\text{def}}{=} \left\langle -\nabla \boldsymbol{P}^{(1)} + \Delta \mathbf{U}^{(1)} - \nabla_c \cdot \left( \mathbf{M} \cdot \langle \mathbf{M} \rangle^{-1} \right) \right\rangle . \tag{3.38}$$

As usual, this system is integro-differential (here because of $\mathbf{N}$) and we can simplify it using the decomposition

$$\boldsymbol{P}^{(1)} = \boldsymbol{P}^{(1)*} + \mathbf{g} \cdot \mathbf{N} \tag{3.39a}$$

$$\mathbf{U}^{(1)} = \mathbf{U}^{(1)*} + \mathbf{G} \cdot \mathbf{N} \tag{3.39b}$$

with $(\mathbf{g},\ \mathbf{G})$ solving Eqs 3.15a and $\left(\boldsymbol{P}^{(1)*},\ \mathbf{U}^{(1)*}\right)$ solving

$$0 = -\nabla \boldsymbol{P}^{(1)*} + \Delta \mathbf{U}^{(1)*} - \nabla_c \cdot \left( \mathbf{M} \cdot \langle \mathbf{M} \rangle^{-1} \right) \qquad \text{in } \Omega_f^{\text{u-c}} \tag{3.40a}$$

$$0 = \nabla \cdot \mathbf{U}^{(1)*} \qquad \text{in } \Omega_f^{\text{u-c}} \tag{3.40b}$$

$$\mathbf{U}^{(1)*} = 0 \qquad \text{on } \Gamma_{fs}^{\text{u-c}} \tag{3.40c}$$

$$\text{Periodicity} \qquad \text{on } \Gamma_{fe}^{\text{u-c}} \tag{3.40d}$$

$$\text{Average } \left\langle \boldsymbol{P}^{(1)*} \right\rangle = 0 \tag{3.40e}$$

Using $\left\langle \mathbf{U}^{(1)} \right\rangle = 0$ , we have that

$$\mathbf{N} = -\langle \mathbf{G} \rangle^{-1} \cdot \left\langle \mathbf{U}^{(1)*} \right\rangle . \tag{3.41}$$

We also define $\mathbf{N}^*$ as

$$\mathbf{N}^* \overset{\text{def}}{=} -\phi \langle \mathbf{G} \rangle \cdot \mathbf{N} = \mathbf{K} \cdot \mathbf{N} = \phi \left\langle \mathbf{U}^{(1)*} \right\rangle \tag{3.42}$$

Introducing Eq 3.36 into Eq 3.31, we obtain the macroscale equation

$$\left\langle \mathbf{u}^{(1)} \right\rangle^D = \mathbf{K} \cdot \left( -\nabla \left\langle p^{(1)} \right\rangle + \frac{\beta^\star}{Wi} \nabla_c \cdot \left\langle \mathbf{c}^{(0)} \right\rangle \right) - \frac{\beta^\star}{Wi} \mathbf{N}^* \cdot \left\langle \mathbf{c}^{(0)} \right\rangle . \tag{3.43}$$

*3.5. Summary*

Summing up the equations for momentum transport at different orders, considering the leading order transport for the conformation tensor and removing the $\varepsilon$ for simplicity, we get

$$\langle \mathbf{u} \rangle^D = \mathbf{K} \cdot \left( -\nabla \langle p \rangle^f + \mathbf{F} + \frac{\beta}{Wi} \nabla_c \cdot \left\langle \mathbf{c}^{(0)} \right\rangle^f \right) - \frac{\beta}{Wi} \mathbf{N}^* \cdot \left\langle \mathbf{c}^{(0)} \right\rangle \tag{3.44a}$$

$$\left\langle \mathbf{u}^{(0)} \right\rangle^D = \mathbf{K} \cdot \left( -\nabla \left\langle p^{(0)} \right\rangle^f + \mathbf{F} \right) \tag{3.44b}$$

$$\nabla \cdot \langle \mathbf{u} \rangle^D = \nabla \cdot \left\langle \mathbf{u}^{(0)} \right\rangle^D = 0 \tag{3.44c}$$

$$\partial_t \left\langle \mathbf{c}^{(0)} \right\rangle + \phi^{-1} \left\langle \mathbf{u}^{(0)} \right\rangle^D \cdot \nabla \left\langle \mathbf{c}^{(0)} \right\rangle = \mathbf{B} \cdot \left\langle \mathbf{c}^{(0)} \right\rangle - \frac{1}{Wi} \left( \left\langle \mathbf{c}^{(0)} \right\rangle - \mathbf{i} \right) \tag{3.44d}$$

with

$$\mathbf{K} = -\phi \left\langle \mathbf{G} \right\rangle, \tag{3.45a}$$

$$\mathbf{N}^* = \phi \left\langle \mathbf{U}^{(1)*} \right\rangle, \tag{3.45b}$$

$$\mathbf{B} = \frac{1}{Wi} \left( \mathbf{I}_{\frac{d(d+1)}{2}} - \left\langle \mathbf{M} \right\rangle^{-1} \right). \tag{3.45c}$$

The corresponding closure problems are

$$0 = -\nabla \mathbf{g} + \Delta \mathbf{G} - \mathbf{I}_d \qquad \text{in } \Omega_f^{\text{u-c}} \tag{3.46a}$$

$$0 = \nabla \cdot \mathbf{G} \qquad \text{in } \Omega_f^{\text{u-c}} \tag{3.46b}$$

$$\mathbf{G} = 0 \qquad \text{on } \Gamma_{fs}^{\text{u-c}} \tag{3.46c}$$

$$\text{Periodicity} \qquad \text{on } \Gamma_{fe}^{\text{u-c}} \tag{3.46d}$$

$$\text{Average } \langle \mathbf{g} \rangle = 0 \tag{3.46e}$$

and

$$\mathbf{u}^{(0)} \cdot \nabla \mathbf{M} = D\mathbf{u}^{(0)} \cdot \mathbf{M} - \frac{1}{Wi} \left( \mathbf{M} - \mathbf{I}_{\frac{d(d+1)}{2}} \right) \qquad \text{in } \Omega_f^{\text{u-c}} \tag{3.47a}$$

$$\text{Periodicity} \qquad \text{on } \Gamma_{fe}^{\text{u-c}} \tag{3.47b}$$

and

$$0 = -\nabla \boldsymbol{P}^{(1)*} + \Delta \mathbf{U}^{(1)*} - \nabla_c \cdot \left( \mathbf{M} \cdot \left\langle \mathbf{M} \right\rangle^{-1} \right) \qquad \text{in } \Omega_f^{\text{u-c}} \tag{3.48a}$$

$$0 = \nabla \cdot \mathbf{U}^{(1)*} \qquad \text{in } \Omega_f^{\text{u-c}} \tag{3.48b}$$

$$\mathbf{U}^{(1)*} = 0 \qquad \text{on } \Gamma_{fs}^{\text{u-c}} \tag{3.48c}$$

$$\text{Periodicity} \qquad \text{on } \Gamma_{fe}^{\text{u-c}} \tag{3.48d}$$

$$\text{Average } \left\langle \boldsymbol{P}^{(1)*} \right\rangle = 0 \tag{3.48e}$$

## 4. Test cases

In this section, we study two test cases corresponding to flows in a channel and through arrays of cylinders. We aim at validating our approach by comparison with either analytical solutions in the case of channel flow or direct numerical simulations in the case of the cylinders. We also use these test cases to evaluate further the model, for instance by calculating how the effective parameters vary with the Weissenberg number.

*4.1. Channel flow*

Let us consider a steady two-dimensional flow between the two lines $y = 0$ and $y = 1$ with no-slip boundary conditions. We further suppose that the flow is periodic in the $x$ direction and is imposed through a force $\mathbf{F} = \begin{pmatrix} 1 & 0 \end{pmatrix}^{\mathsf{T}}$. The reference analytical solution of this problem is given by

$$\mathbf{u}_{\text{ref}} = \begin{pmatrix} \frac{1}{2}\frac{y(1-y)}{(1+\beta)} \\ 0 \end{pmatrix} \tag{4.1}$$

and

$$\mathbf{c}_{\text{ref}} = \begin{pmatrix} 1 + \frac{Wi^2}{2}\frac{(1-2y)^2}{(1+\beta)^2} \\ 1 \\ \frac{Wi}{2}\frac{(1-2y)}{1+\beta} \end{pmatrix}. \tag{4.2}$$

Through asymptotics in $\beta$, we then have

$$\mathbf{u}^{(0)}_{\text{ref}} = \begin{pmatrix} \frac{1}{2}y\,(1-y) \\ 0 \end{pmatrix} \tag{4.3}$$

and

$$\mathbf{u}^{(1)}_{\text{ref}} = \beta \begin{pmatrix} -\frac{1}{2}y\,(1-y) \\ 0 \end{pmatrix} \tag{4.4}$$

and

$$\mathbf{c}^{(0)}_{\text{ref}} = \begin{pmatrix} 1 + \frac{Wi^2}{2}\,(1-2y)^2 \\ 1 \\ \frac{Wi}{2}\,(1-2y) \end{pmatrix} \tag{4.5}$$

Averaging these equations, we obtain

$$\left\langle \mathbf{u}^{(0)}_{\text{ref}} \right\rangle = \begin{pmatrix} 1/12 \\ 0 \end{pmatrix}, \tag{4.6}$$

and

$$\left\langle \mathbf{u}^{(1)}_{\text{ref}} \right\rangle = \beta \begin{pmatrix} -1/12 \\ 0 \end{pmatrix}, \tag{4.7}$$

and

$$\left\langle \mathbf{c}^{(0)}_{\text{ref}} \right\rangle = \begin{pmatrix} 1 + \frac{1}{6}Wi^2 \\ 1 \\ 0 \end{pmatrix}. \tag{4.8}$$

*Solution of the homogenized formulation.* Now that we have reference analytical solutions, we proceed to calculating the result of our homogenized formulation. $\mathbf{G}$ solves Eq 3.46 and can be easily calculated as

$$\mathbf{G} = \begin{pmatrix} -\frac{1}{2}y\,(1-y) & 0 \\ 0 & 0 \end{pmatrix}. \tag{4.9}$$

We then have

$$\mathbf{K} = -\langle \mathbf{G} \rangle = \begin{pmatrix} 1/12 & 0 \\ 0 & 0 \end{pmatrix} \tag{4.10}$$

and $\left\langle \mathbf{u}^{(0)} \right\rangle = \mathbf{K} \cdot \mathbf{F}$ leading to

$$\left\langle \mathbf{u}^{(0)} \right\rangle = \begin{pmatrix} 1/12 \\ 0 \end{pmatrix} = \left\langle \mathbf{u}^{(0)}_{\text{ref}} \right\rangle. \tag{4.11}$$

We thus recover the correct average velocity.

For the conformation tensor, the problem for $\mathbf{M}$ is

$$0 = D\mathbf{u}^{(0)} \cdot \mathbf{M} - \frac{1}{Wi}\left(\mathbf{M} - \mathbf{I}_{\frac{d(d+1)}{2}}\right) \tag{4.12}$$

so that

$$\mathbf{M} = \left(\mathbf{I}_{\frac{d(d+1)}{2}} - Wi\ D\mathbf{u}^{(0)}\right)^{-1} = \begin{pmatrix} 1 & \frac{1}{2}Wi^2\,(1-2y)^2 & Wi\,(1-2y) \\ 0 & 1 & 0 \\ 0 & \frac{1}{2}Wi\,(1-2y) & 1 \end{pmatrix}. \tag{4.13}$$

By averaging, we obtain

$$\langle \mathbf{M} \rangle = \begin{pmatrix} 1 & \frac{1}{6}Wi^2 & 0 \\ 0 & 1 & 0 \\ 0 & 0 & 1 \end{pmatrix} \tag{4.14}$$

and thus

$$\langle \mathbf{M} \rangle^{-1} = \begin{pmatrix} 1 & -\frac{1}{6}Wi^2 & 0 \\ 0 & 1 & 0 \\ 0 & 0 & 1 \end{pmatrix}. \tag{4.15}$$

We finally have

$$\mathbf{B} = Wi^{-1}\left(\mathbf{I}_{\frac{d(d+1)}{2}} - \langle \mathbf{M} \rangle^{-1}\right) = \begin{pmatrix} 0 & \frac{1}{6}Wi & 0 \\ 0 & 0 & 0 \\ 0 & 0 & 0 \end{pmatrix}, \tag{4.16}$$

and $\left\langle \mathbf{c}^{(0)} \right\rangle$ is given by

$$\left\langle \mathbf{c}^{(0)} \right\rangle = \left(\mathbf{I}_{\frac{d(d+1)}{2}} - Wi\mathbf{B}\right)^{-1} \cdot \mathbf{i}. \tag{4.17}$$

We further have

$$\left(\mathbf{I}_{\frac{d(d+1)}{2}} - Wi\mathbf{B}\right)^{-1} = \begin{pmatrix} 1 & \frac{1}{6}Wi^2 & 0 \\ 0 & 1 & 0 \\ 0 & 0 & 1 \end{pmatrix} \tag{4.18}$$

so that

$$\left\langle \mathbf{c}^{(0)} \right\rangle = \begin{pmatrix} 1 + \frac{1}{6} Wi^2 \\ 1 \\ 0 \end{pmatrix} = \left\langle \mathbf{c}_{\text{ref}}^{(0)} \right\rangle, \tag{4.19}$$

and we also recover the exact solution.

Let us now consider the first-order correction to the velocity. We want to solve Eq 3.48 so that we first need to evaluate $\mathbf{M} \cdot \langle \mathbf{M} \rangle^{-1}$. Using Eqs 4.14 and 4.15, we have

$$\mathbf{M} \cdot \langle \mathbf{M} \rangle^{-1} = \begin{pmatrix} 1 & -\frac{1}{6} Wi^2 + \frac{1}{2} Wi^2 (1-2y)^2 & Wi\,(1-2y) \\ 0 & 1 & 0 \\ 0 & \frac{1}{2} Wi\,(1-2y) & 1 \end{pmatrix} \tag{4.20}$$

We can then calculate

$$-\nabla_c \cdot \left( \mathbf{M} \cdot \langle \mathbf{M} \rangle^{-1} \right) = \begin{pmatrix} 0 & Wi & 0 \\ 0 & 0 & 0 \end{pmatrix} \tag{4.21}$$

Solving Eq 3.48 then leads to

$$\mathbf{U}^{(1)*} = \begin{pmatrix} 0 & \frac{1}{2} y\,(1-y)\, Wi & 0 \\ 0 & 0 & 0 \end{pmatrix} \tag{4.22}$$

By averaging, we have

$$\left\langle \mathbf{U}^{(1)*} \right\rangle = \mathbf{N}^* = \begin{pmatrix} 0 & \frac{1}{12} Wi & 0 \\ 0 & 0 & 0 \end{pmatrix} \tag{4.23}$$

Finally, Eq 3.43

$$\left\langle \mathbf{u}^{(1)} \right\rangle = \frac{\beta}{We} \mathbf{K} \cdot \left( \nabla_c \cdot \left\langle \mathbf{c}^{(0)} \right\rangle \right) - \frac{\beta}{Wi} \mathbf{N}^* \cdot \left\langle \mathbf{c}^{(0)} \right\rangle \tag{4.24}$$

with

$$\nabla_c \cdot \left\langle \mathbf{c}^{(0)} \right\rangle = \begin{pmatrix} 0 \\ 0 \end{pmatrix} \tag{4.25}$$

and

$$-\mathbf{N}^* \cdot \left\langle \mathbf{c}^{(0)} \right\rangle = \begin{pmatrix} -\frac{1}{12} Wi \\ 0 \end{pmatrix} \tag{4.26}$$

leads to

$$\left\langle \mathbf{u}^{(1)} \right\rangle = \beta \begin{pmatrix} -\frac{1}{12} \\ 0 \end{pmatrix} = \left\langle \mathbf{u}_{\text{ref}}^{(1)} \right\rangle. \tag{4.27}$$

*4.2. Flow through biperiodic arrays of cylinders*

We now turn to arrays of cylinders with both crystalline and amorphous structures – amorphous structures generated by randomly displacing cylinders from the crystalline structure,

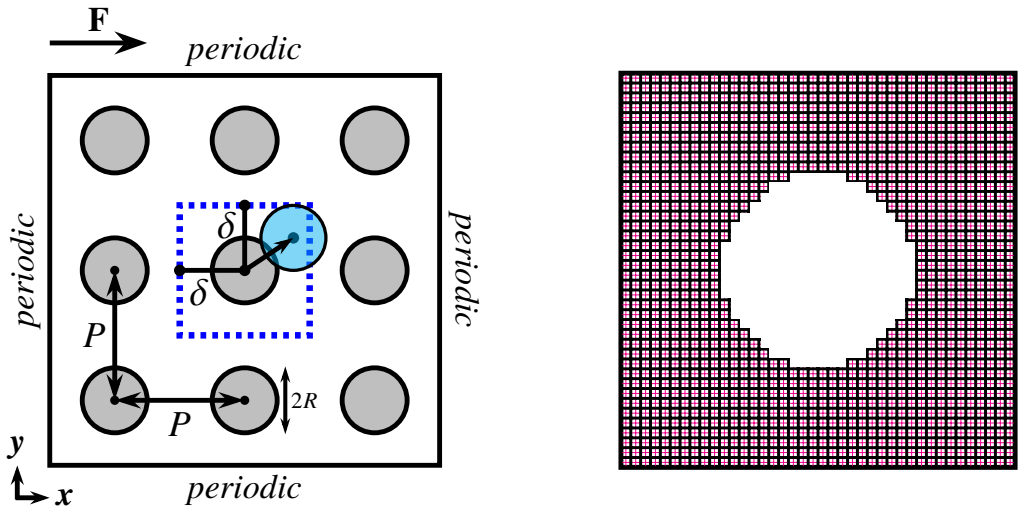


(a) Geometry (b) Mesh

Figure 4.1: Geometry and mesh for simulations through biperiodic arrays. The crystalline structure corresponds to the grey circles of radius $R$ with distance $P$ between the centers of the circles. *The amorphous structures* are obtained by randomly displacing each circle. Each component of the displacement vector is obtained by uniform random sampling of the interval $[0, \varepsilon]$. The mesh is Cartesian and consists of $N \times N$ square cells of equal size. The cells are taken as holes if they are cut by the cylinder. An example of a mesh for a single cylinder is given in (b) in the case $N = 40$. This mesh is refined by splitting each face into 2 equal parts, which amounts to splitting each cell into 4 parts.

as detailed in Fig 4.1. We consider steady biperiodic flow. We can eliminate gradients of average quantities because of the periodicity and the macroscale model simply boils down to

$$\frac{\langle \mathbf{u} \rangle^D - \langle \mathbf{u}^{(0)} \rangle^D}{\beta} = -\frac{1}{Wi} \mathbf{N}^* \cdot \langle \mathbf{c}^{(0)} \rangle \tag{4.28a}$$

$$0 = \mathbf{B} \cdot \langle \mathbf{c}^{(0)} \rangle - \frac{1}{Wi} \left( \langle \mathbf{c}^{(0)} \rangle - \mathbf{i} \right) \tag{4.28b}$$

Calculating $\langle \mathbf{c}^{(0)} \rangle = \left( \mathbf{I}_{\frac{d(d+1)}{2}} - Wi \mathbf{B} \right)^{-1} \cdot \mathbf{i}$ from the second equation and injecting it in the first one, we further get

$$\frac{\langle \mathbf{u} \rangle^D - \langle \mathbf{u}^{(0)} \rangle^D}{\beta} = -\mathbf{N}^* \cdot \left( Wi \, \mathbf{I}_{\frac{d(d+1)}{2}} - Wi^2 \mathbf{B} \right)^{-1} \cdot \mathbf{i}, \tag{4.29}$$

that can also be written as

$$\frac{\langle \mathbf{u} \rangle^D - \langle \mathbf{u}^{(0)} \rangle^D}{\beta} = -\frac{1}{Wi} \mathbf{N}^* \cdot \langle \mathbf{M} \rangle \cdot \mathbf{i}. \tag{4.30}$$

In this case, the caracteristic lengthscale used to determine the $Wi$ number is $H = P - 2R$, which corresponds to the smallest distance between the surfaces of two successive circles.

*4.2.1. Numerical methods*

The aim is to solve both the Oldroyd-B problem Eq 2.2 and the closure problems Eqs 3.46, 3.47 and 3.48. Our numerical approach follows that developed and detailed in [34]. The space discretization relies on a partition of the domain with quadrilateral cells and consists in a staggered approximation of the unknowns with nonconforming low-order finite elements, namely the Rannacher and Turek (RT) element. The discrete unknowns of $\mathbf{u}$, $\mathsf{G}$ and $\mathsf{U}^{(1)*}$ are located at the center of the faces of the mesh while the discrete unknowns of $\mathsf{C}$ and $\mathsf{M}$ are associated with the cells of the mesh. $\mathsf{C}$ and $\mathsf{M}$ are discretized as piecewise constant and the corresponding transport equations are then solved using a finite-volume scheme.

We use a mesh that is structured and uniform, consisting of $N \times N$ square cells of equal size. Circles are approximated as "stair steps" by making holes into the mesh. In order to keep the geometry unchanged, mesh refinement is obtained by cutting each face into 2 equal parts and each cell into $2 \times 2$ parts. An exemple of the mesh for a single circle is given Fig 4.1 in the case $N = 40$. We used a constant mesh size with $N = 100$, corresponding to a characteristic cell size of $1/50$ radius of a circle. In all the computations, steady-state is obtained by running a transient computation until the solution stabilizes in time. The time step is monitored to ensure time convergence towards steady-state solutions.

*Decoupling of the Oldroyd-B problem.* The scheme is based upon a fractional step approach. Hydrodynamics equations (i.e. mass and momentum balance equations) are decoupled from the constitutive equation by using a beginning-of-step approximation $\mathsf{C}^n$ of the conformation tensor in the momentum balance equation. The problem then consists of iteratively solving a Stokes system

$$0 = -\nabla p + \Delta \mathbf{u} + \frac{\beta}{Wi} \nabla_c \cdot \mathsf{C}^n + \mathbf{F}, \tag{4.31a}$$

$$0 = \nabla \cdot \mathbf{u}, \tag{4.31b}$$

with no-slip/no-penetration boundary conditions on solid interfaces and a transport equation of the conformation tensor

$$\partial_t \mathsf{C}^{n+1} + \mathbf{u} \cdot \nabla \mathsf{C}^{n+1} = \nabla \mathbf{u} \cdot \mathsf{C}^{n+1} + \mathsf{C}^{n+1} \cdot \nabla (\mathbf{u})^{\mathsf{T}} - \frac{1}{Wi} \left( \mathsf{C}^{n+1} - \mathsf{I}_d \right). \tag{4.32}$$

*Solution of the Stokes problems.* Systems 4.31, 3.46, and 3.48 can all be written as a Stokes problem

$$0 = -\nabla h + \Delta \mathbf{H} + \mathbf{S}, \tag{4.33a}$$

$$0 = \nabla \cdot \mathbf{H}, \tag{4.33b}$$

with the scalar $h$ and the vector $\mathbf{H}$ as unknowns and the vector $\mathbf{S}$ as (volumic) source term. These systems are solved in an iterative manner. A standard projection scheme is used to decouple the momentum balance equation from the divergence constraint, thus making it

possible to avoid solving a discrete saddle point problem. The solution is obtained by the following algorithm

$$
\begin{aligned}
&\text{While } \|\mathbf{H}^{k+1}-\mathbf{H}^{k}\|_{\infty} > tol :\\
&\quad \textbf{Prediction step} - \text{Solve for } \tilde{\mathbf{H}}^{k+1} :\\
&\quad \frac{1}{dt}\left(\tilde{\mathbf{H}}^{k+1}-\mathbf{H}^{k}\right) + \nabla h^{k} - \nabla\cdot\left(\nabla\tilde{\mathbf{H}}^{k+1} + \left(\nabla\tilde{\mathbf{H}}^{k+1}\right)^{\mathsf{T}}\right) + \mathbf{S} = 0.\\
&\quad \textbf{Correction step} - \text{Solve for } h^{k+1} \text{ and } \mathbf{H}^{k+1} :\\
&\quad \frac{1}{dt}\left(\mathbf{H}^{k+1}-\tilde{\mathbf{H}}^{k+1}\right) + \nabla\left(h^{k+1}-h^{k}\right) = 0,\\
&\quad \nabla\cdot\mathbf{H}^{k+1} = 0,
\end{aligned}
$$

where $dt$ is the time step and the tolerance $tol$ is fixed here to $10^{-6}$.

*Solution of the transport problems.* The time discretization of the conformation transport $\mathbf{C}$ is performed using a Strang-type decoupling. A half-step of homogeneous transport of $\mathbf{C}$ is first performed. Then we treat the reaction terms, and finish by the second half-step of transport of $\mathbf{C}$. For precision, we introduce a log transformation of the conformation tensor (see [14, 23]) that is applied to the transport equation. The scheme reads

$$
\begin{aligned}
&\textbf{Advection I} - \text{Solve for } \mathbf{C}^{n+\frac{1}{3}} :\\
&\quad \frac{1}{dt/2}\left(\log\,\mathbf{C}^{n+\frac{1}{3}} - \log\,\mathbf{C}^{n}\right) + \nabla\cdot\left(\boldsymbol{u}^{n+1}\log\,\mathbf{C}^{n+\frac{1}{3}}\right) = 0.\\
&\textbf{ODE} - \text{Set } \mathbf{C}(t_n) = \mathbf{C}^{n+\frac{1}{3}} \text{ and solve for } \mathbf{C}^{n+\frac{2}{3}} = \mathbf{C}(t_n+dt) :\\
&\quad \dot{\mathbf{C}} - \left(\nabla\boldsymbol{u}^{n+1}\right)\mathbf{C} - \mathbf{C}^{\mathsf{T}}\left(\nabla\boldsymbol{u}^{n+1}\right)^{\mathsf{T}} + \frac{1}{Wi}\left(\mathbf{C}-\mathbf{I}\right) = 0.\\
&\textbf{Advection II} - \text{Solve for } \mathbf{C}^{n+1} :\\
&\quad \frac{1}{dt/2}\left(\log\,\mathbf{C}^{n+1} - \log\,\mathbf{C}^{n+\frac{2}{3}}\right) + \nabla\cdot\left(\boldsymbol{u}^{n+1}\log\,\mathbf{C}^{n+1}\right) = 0.
\end{aligned}
$$

The matrix $\mathbf{C}$ being symmetric positive definite, there exists an invertible matrix $\boldsymbol{P}\in\mathbb{R}^{d\times d}$ and $\lambda_1,\ldots,\lambda_d\in\mathbb{R}^{+*}$ such that $\mathbf{C} = \boldsymbol{P}^{-1}diag(\lambda_1,\ldots,\lambda_d)\boldsymbol{P}$. The log transformation of $\mathbf{C}$ is then defined by $\log\,\mathbf{C} = \boldsymbol{P}^{-1}diag\left(\log(\lambda_1),\ldots,\log(\lambda_d)\right)\boldsymbol{P}$.

The local ODE is solved using a first-order implicit Euler scheme

$$
\begin{cases}
\mathbf{C}_0 & = \mathbf{C}^{n},\\
\frac{1}{\delta t}\left(\mathbf{C}_{k+1}-\mathbf{C}_{k}\right) & = \nabla\boldsymbol{u}^{n+1}\,\mathbf{C}_{k+1} + \left(\mathbf{C}_{k+1}\right)^{\mathsf{T}}\left(\nabla\boldsymbol{u}^{n+1}\right)^{\mathsf{T}} - \frac{1}{Wi}\left(\mathbf{C}_{k+1}-\mathbf{I}\right),
\end{cases}
$$

where $\delta t$ is a local time-step for the solution of the ODE on each mesh element. To preserve the positive definiteness of the conformation tensor, this local time-step for the solution of the ODE is set to $\delta t = {}^{dt}/_{n}$ with $n$ the smallest integer number such that $\delta t \leq 1/\left(100\|\nabla u^{n+1}\|_{\infty}\right)$, see [34].

For $\mathbf{M}$, we proceed exactly as for $\mathbf{C}$ by considering the unsteady form of the transport problem Eq 3.47

$$\partial_t \mathbf{M} + \mathbf{u}^{(0)} \cdot \nabla \mathbf{M} = D\mathbf{u}^{(0)} \cdot \mathbf{M} - \frac{1}{We}\left(\mathbf{M} - \mathbf{I}_{\frac{d(d+1)}{2}}\right) \tag{4.34a}$$

$$\mathbf{M}_{(t=0)} = \mathbf{I}_{\frac{d(d+1)}{2}} \tag{4.34b}$$

and wait until steady-state is reached. The matrix is no longer symmetric but remains positive definite. The computation of the logarithm is then done by a block diagonalization which consists in computing the Schur form and to eliminate off-diagonal blocks by solving Sylvester equations [8].

*Implementation and high performance computing.* The solvers are implemented as specific modules of the CALIF$^3$S platform [1] developed at the French Institut de Radioprotection et de Sûreté Nucléaire (IRSN). Parallel computations were carried out on TotalEnergies' group supercomputer Pangea II through a domain decomposition approach using the OpenMPI (3.1.5) library [15] and the METIS (4.0.3) graph partitioner [26]. All the linear systems are preconditionned by a Block-Jacobi preconditioner. The linear systems coming from the prediction steps and the transport problems are solved using the GMRES method [41]. The projection steps are solved using a classical conjugate gradient method. The log transformation of the conformation tensor is done by diagonalizing $\mathbf{C}$, using a QR decomposition. The log transformation of $\mathbf{M}$ is carried out using the Eigen (3.4.0) library [16]. Finally, the linear systems coming from the local ODE are solved using a direct LU method.

### *4.2.2. Results*

We plot in Fig 4.2a and Fig 4.2b the components of the matrices $\mathbf{B}$ and $\mathbf{N}^*$ for the crystalline case. The dominant terms are $B_{12}$ and $\mathsf{N}^*_{12}$, which is similar to the channel flow. This is because of the structure of the birefringent strands and the flow in this case. As discussed in Harlen [17], Mokhtari et al. [35], Rallison and Hinch [40], the strands follow streamlines and can be thought of as a line distribution of forces in an otherwise Newtonian fluid. In the crystalline case, strands connect the circles on both sides and a large channel flow develops between lines of circles, see Fig 4.3. Because of this structure, the situation is actually close to the channel flow and dominant terms in the $\mathbf{B}$ and $\mathbf{N}^*$ are the same. It is also important to note that, although $B_{11}$ is much smaller, it still is important with the increase in $C^{(0)}_{xx}$ being controlled by $B_{11}C^{(0)}_{xx} + B_{12}C^{(0)}_{yy}$. Similarly, the additional drag due to viscoelasticity is primarily determined by both $N^*_{11}$ and $N^*_{12}$ .

To assess the validity of our approach and its limits, we plot in Figs 4.2c and 4.2d the normalized trace of the conformation tensor and the average velocity for both the homogenized model and the average results of the direct numerical simulations for different values of $\beta$. We see that the homogenized model is, as expected, valid in the limit $\beta \ll 1$ with our approach providing a reasonable approximation up to $\beta \simeq 10^{-1}$. Beyond $\beta \simeq 10^{-1}$, the overall trend is similar but the feedback of the strands upon the flow field becomes too important and higher-order terms would be needed to obtain a more accurate representation.

We now turn to the case of a flow in an amorphous structure, with example fields for the conformation tensor and the velocity shown in Fig 4.4 at different values of $\beta$. The strands

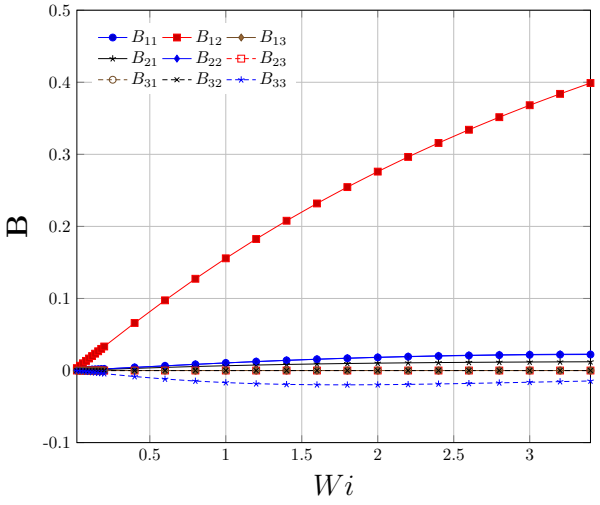


(a) **B** as a function of $Wi$

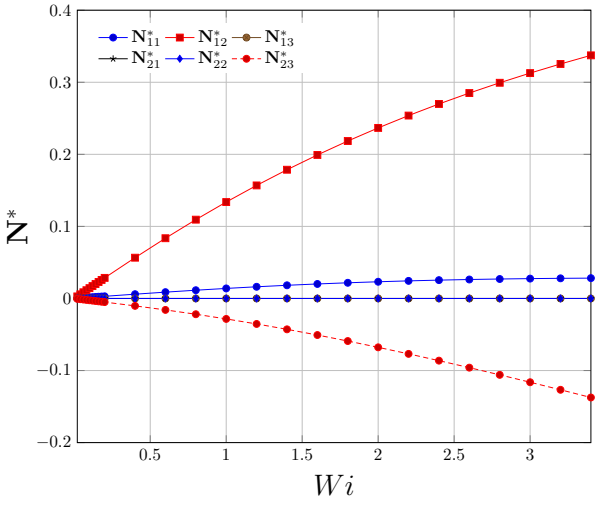


(b) $\mathbf{N}^*$ as a function of $Wi$

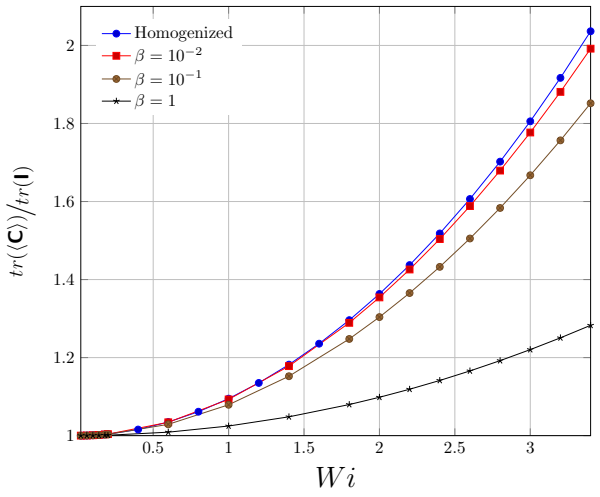


(c) Normalized trace of **C** as a function of $Wi$

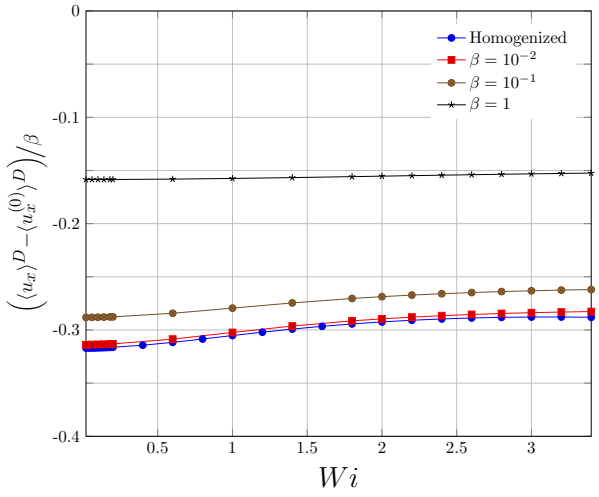


(d) Normalized velocity as a function of $Wi$

Figure 4.2: Crystalline structure: components of the effective matrices in the homogenized models and comparison between homogenized and direct numerical simulations for different values of $\beta$.

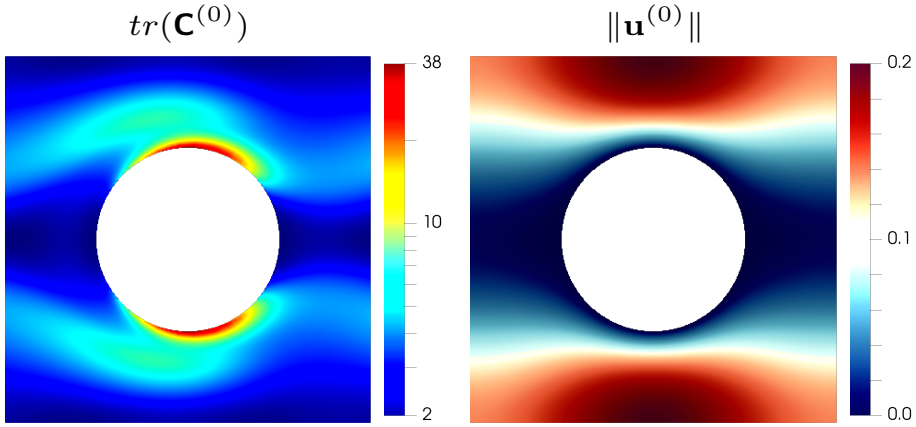


Figure 4.3: Example of fields obtained for $tr\left(\mathbf{C}^{(0)}\right)$ and $\left\|\mathbf{u}^{(0)}\right\|$ in the crystalline structure at $Wi = 3.4$. We observe, in the $tr\left(\mathbf{C}^{(0)}\right)$ field, the formation of an envelope that encompasses the cylinder and delimits a low velocity zone upstream and downstream of the cylinder.

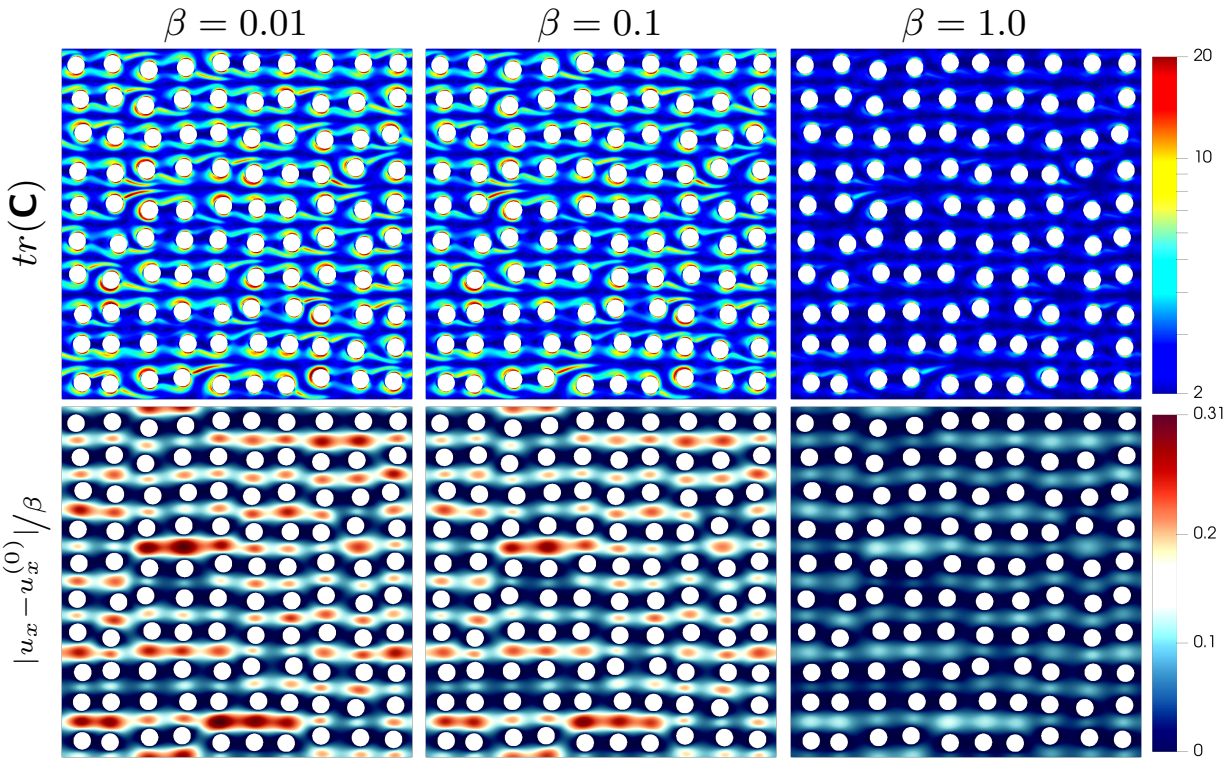


Figure 4.4: Trace of the conformation tensor and velocity fields for the amorphous structure ($\delta = 0.5$) at $Wi = 3.4$.

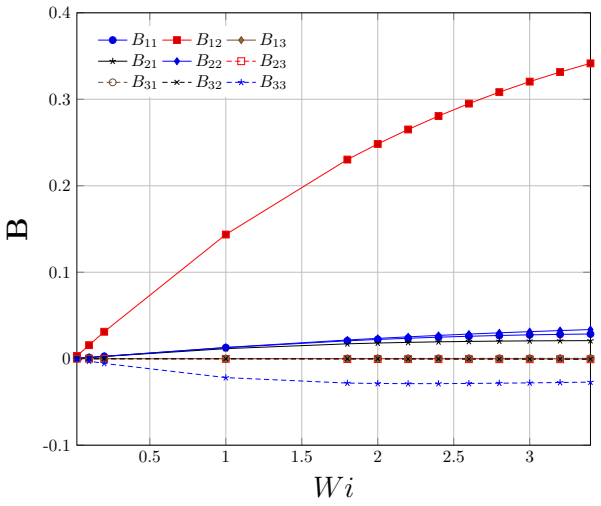


(a) **B** as a function of $Wi$

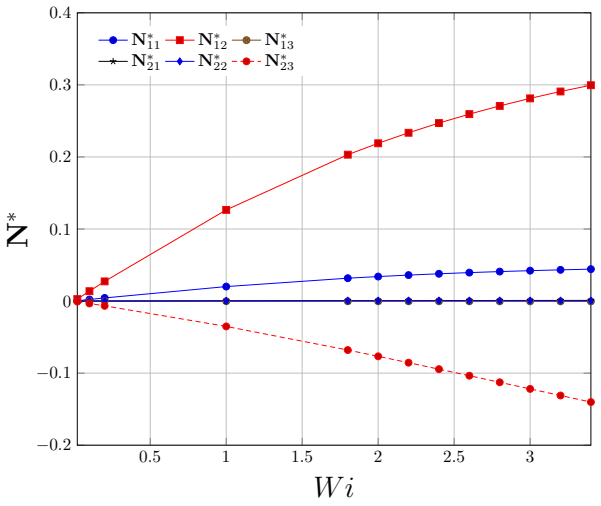


(b) $\mathbf{N}^*$ as a function of $Wi$

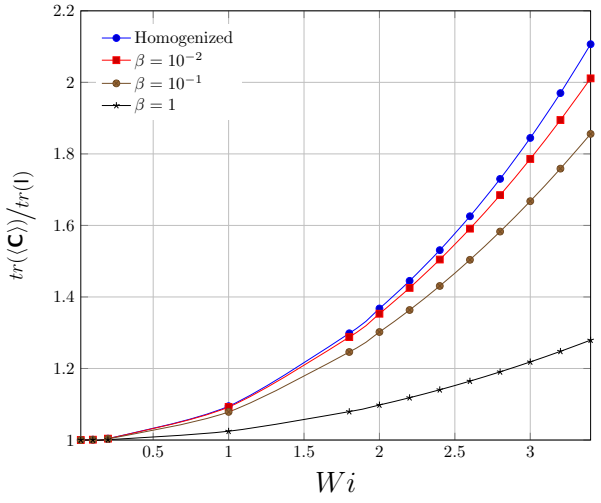


(c) Normalized trace of **C** as a function of $Wi$

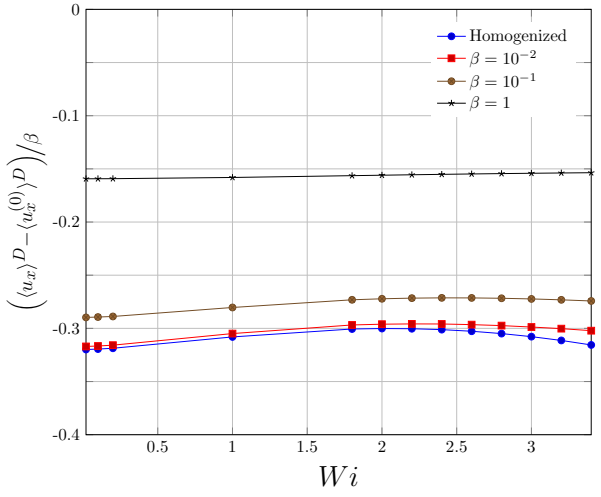


(d) Normalized velocity as a function of $Wi$

Figure 4.5: Amorphous structure ($\delta = 0.5$): components of the effective matrices in the homogenized models and comparison between homogenized and direct numerical simulations for different values of $\beta$.

show clearly in the wake of each circle at $\beta = 10^{-2}$ and $\beta = 10^{-1}$. $\beta = 1$ is associated with a stronger coupling between momentum and transport of the conformation tensor with both a decrease in the intensity of the strands and the velocity magnitude. In Figs 4.5a and 4.5b, we plot the components of matrices $\mathbf{B}$ and $\mathbf{N}^*$. Again, $B_{12}$ and $\mathsf{N}^*_{12}$ are the dominant components but are relatively weaker compared to the crystalline case. We further compare direct numerical simulations of the Oldroyd-B model with the homogenized model in Figs 4.5c and 4.5d. These results show again that our approach yields a reasonable appoximation up to $\beta \simeq 10^{-1}$. We also see that the behaviour of the velocity difference is non-monotonic with the Weissenberg number. Such apparent thinning, followed by apparent thickening, is a known phenomenon in the flow of polymer solutions through porous media [5, 20]. We have hypothesized in Mokhtari et al. [35] that, for steady flows, this is due to the presence of the birefringent strands. Interestingly, our homogenized model is able to capture this phenomenon.

Figs 4.6a and 4.6b show the $xx$ and $yy$ components of the conformation tensor for the solution of the homogenized model in all the different structure. We recover a solution for $C^{(0)}_{xx}$ that is very close to the channel flow in all different structures, even though the components of $\mathbf{B}$ vary significantly (see Figs 4.6c). The primary difference is for $C^{(0)}_{yy}$. $C^{(0)}_{yy} = 0$ for the channel case but is non-zero for all other cases and seems to increase with the "disorder" in the structure.

## 5. Conclusions

We have developed a homogenized model for the flow of an Oldroyd-B fluid through porous media. The model consists of an advection-reaction transport equation for the average conformation tensor along with a Darcy's law containing an additional drag generated by viscoleastic stress. It is valid in a limit of high dilutation for polymer solutions. Our simulations and test cases show that we obtain reasonably accurate solutions for sufficiently dilute suspensions. The homogenized model can also capture both apparent shear-thinning and shear-thickening, an important property of the flow of polymer solutions through porous media.

Although the case of high dilution is of course limiting, our model is the first proposition of a homogenized model for viscoelastic flows through porous media that can actually capture the effects of birefringent strands. Our model shows that modeling viscoelastic flows through porous media cannot be reduced to calculating an apparent permeability in a simple Darcy's law. Our model couples a transport equation for the polymeric stress with a modified form of Darcy's law that features an additional drag term associated with stress localization at pore-scale. This suggests that we need specific models for viscoelastic flows through porous media and not just empirical extensions of Darcy's law. Generalizations of our approach to a wider range of flow regimes may be possible, for instance by considering higher-order asymptotics that can describe the feedback of the strands upon the flow field at pore-scale.

*Acknowledgments.* The authors thank R. de Loubens, from TotalEnergies, for valuable discussions and F. Babik, from the CALIF3S development team at IRSN, for his precious

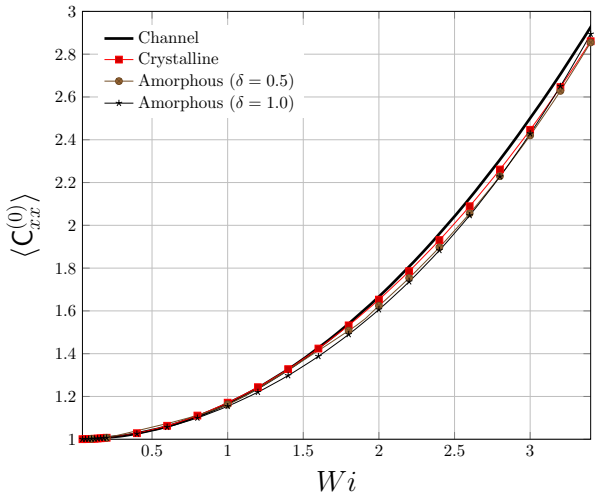


(a) $C_{xx}$ component of the conformation tensor

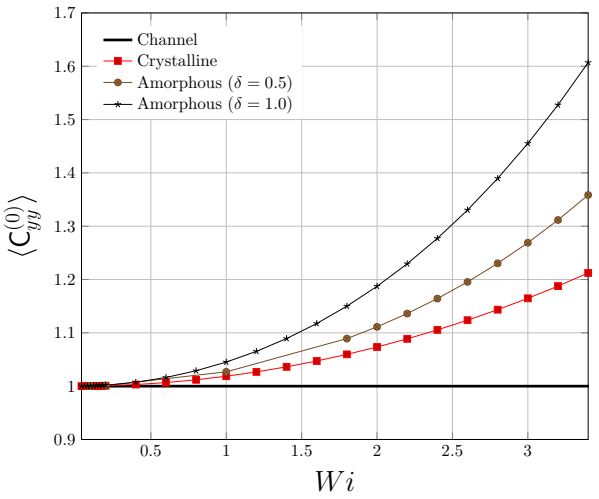


(b) $C_{yy}$ component of the conformation tensor

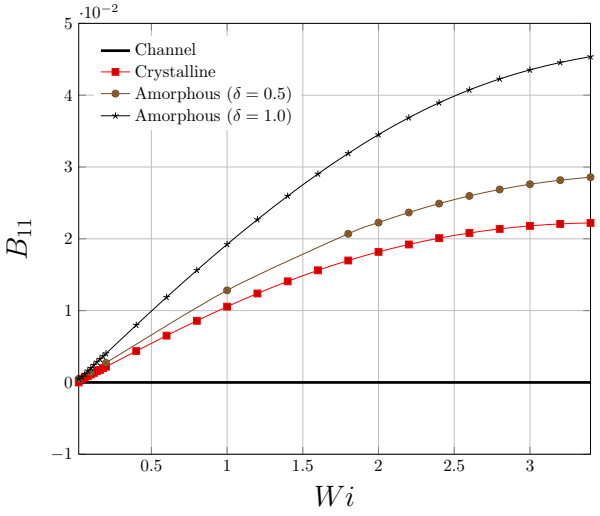


(c) $B_{11}$ as a function of $Wi$

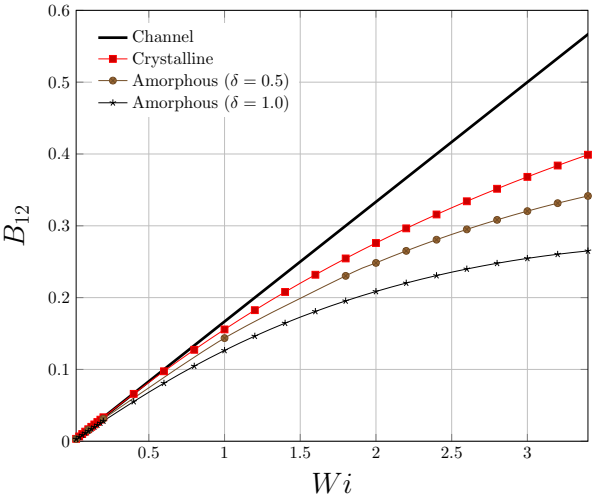


(d) $B_{11}$ as a function of $Wi$

Figure 4.6: Comparisons of the conformation tensor and of the dominant components in the matrix **B** for the different structures.

support. The authors would also like to thank TotalEnergies for funding and supporting this work, in particular through access to the PANGEA II supercomputer.

## References

[1] CALIF3S (1.32). A Computational Fluid Dynamics software based on Pelicans. https://gforge.irsn.fr/gf/project/calif3s, 2021.

[2] F. J. Alcocer and P. Singh. Permeability of periodic arrays of cylinders for viscoelastic flows. *Physics of Fluids*, 14(7):2578–2581, 2002.

[3] R. B. Bird, C. F. Curtiss, R. C. Armstrong, and O. Hassager. *Dynamics of polymeric liquids, volume 2: Kinetic theory*. Wiley, 1987.

[4] D. Bresch and C. Prange. Newtonian limit for weakly viscoelastic fluid flows. *SIAM Journal on Mathematical Analysis*, 46(2):1116–1159, 2014.

[5] G. Chauveteau. Molecular interpretation of several different properties of flow of coiled polymer solutions through porous media in oil recovery conditions. In *SPE Annual Technical Conference and Exhibition*. OnePetro, 1981.

[6] M. J. Crochet and K. Walters. Numerical methods in non-newtonian fluid mechanics. *Annual Review of Fluid Mechanics*, 15(1):241–260, 1983.

[7] M. J. Crochet, A. R. Davies, and K. Walters. *Numerical simulation of non-newtonian flow*. Elsevier, 2012.

[8] P. I. Davies and N. J. Higham. A schur-parlett algorithm for computing matrix functions. *SIAM Journal on Matrix Analysis and Applications*, 25(2):464–485, 2003.

[9] Y. Davit, C. G. Bell, H. M. Byrne, L. A. C. Chapman, L. S. Kimpton, G. E. Lang, K. H. L. Leonard, J. M. Oliver, N. C. Pearson, R. J. Shipley, et al. Homogenization via formal multiscale asymptotics and volume averaging: How do the two techniques compare? *Advances in Water Resources*, 62:178–206, 2013.

[10] S. De, J. A. M. Kuipers, E. A. J. F. Peters, and J. T. Padding. Viscoelastic flow simulations in random porous media. *Journal of Non-Newtonian Fluid Mechanics*, 248: 50–61, 2017.

[11] M. L. De Haro, J. A. P. Del Río, and S. Whitaker. Flow of Maxwell fluids in porous media. *Transport in Porous Media*, 25(2):167–192, 1996.

[12] F. R. B. U. Durst, R. Haas, and B. U. Kaczmar. Flows of dilute hydrolyzed polyacrylamide solutions in porous media under various solvent conditions. *Journal of Applied Polymer Science*, 26(9):3125–3149, 1981.

[13] L. Fast, J. M. Wills, B. Johansson, and O. Eriksson. Elastic constants of hexagonal transition metals: Theory. *Physical Review B*, 51(24):17431, 1995.

[14] R. Fattal and R. Kupferman. Constitutive laws for the matrix-logarithm of the conformation tensor. *Journal of Non-Newtonian Fluid Mechanics*, 123(2-3):281–285, 2004.

[15] R. L. Graham, T. S. Woodall, and J. M. Squyres. Open MPI: A flexible high performance MPI. In *International Conference on Parallel Processing and Applied Mathematics*, pages 228–239. Springer, 2005.

[16] G. Guennebaud, B. Jacob, et al. Eigen (3.4.0). http://eigen.tuxfamily.org, 2010.

[17] O. G. Harlen. High-deborah-number flow of a dilute polymer solution past a sphere falling along the axis of a cylindrical tube. *Journal of Non-Newtonian Fluid Mechanics*, 37(2-3):157–173, 1990.

[18] S. J. Haward, K. Toda-Peters, and A. Q. Shen. Steady viscoelastic flow around high-aspect-ratio, low-blockage-ratio microfluidic cylinders. *Journal of Non-Newtonian Fluid Mechanics*, 254:23–35, 2018.

[19] J.-H. He. Some asymptotic methods for strongly nonlinear equations. *International Journal of Modern Physics B*, 20(10):1141–1199, 2006.

[20] E. J. Hemingway, A. Clarke, J. R. A. Pearson, and S. M. Fielding. Thickening of viscoelastic flow in a model porous medium. *Journal of Non-Newtonian Fluid Mechanics*, 251:56–68, 2018.

[21] E. J. Hinch. *Perturbation Methods*. Cambridge Texts in Applied Mathematics. Cambridge University Press, 1991. doi: 10.1017/CBO9781139172189.

[22] C. C. Hopkins, S. J. Haward, and A. Q. Shen. Purely elastic fluid–structure interactions in microfluidics: implications for mucociliary flows. *Small*, 16(9):1903872, 2020.

[23] M. A. Hulsen, R. Fattal, and R. Kupferman. Flow of viscoelastic fluids past a cylinder at high Weissenberg number: stabilized simulations using matrix logarithms. *Journal of Non-Newtonian Fluid Mechanics*, 127(1):27–39, 2005.

[24] Y. Itin and F. W. Hehl. The constitutive tensor of linear elasticity: its decompositions, cauchy relations, null lagrangians, and wave propagation. *Journal of Mathematical Physics*, 54(4):042903, 2013.

[25] D. D. Joseph, M. Renardy, and J.-C. Saut. Hyperbolicity and change of type in the flow of viscoelastic fluids. *Archive for Rational Mechanics and Analysis*, 87(3):213–251, 1985.

[26] G. Karypis and V. Kumar. A fast and high quality multilevel scheme for partitioning irregular graphs. *SIAM Journal on Scientific Computing*, 20(1):359–392, 1998.

[27] R. Keunings. On the high Weissenberg number problem. *Journal of Non-Newtonian Fluid Mechanics*, 20:209–226, 1986.

[28] R. Keunings. A survey of computational rheology. In *Proceedings of the XIIIth International Congress on Rheology*, volume 1, pages 7–14. British Soc. Rheol, 2000.

[29] S. Khaitan, S. Kalainesan, L. E. Erickson, P. Kulakow, S. Martin, R. Karthikeyan, S. L. L. Hutchinson, L. C. Davis, T. H. Illangasekare, and C. Ng'oma. Remediation of sites contaminated by oil refinery operations. *Environmental Progress*, 25(1):20–31, 2006.

[30] B. Khuzhayorov, J.-L. Auriault, and P. Royer. Derivation of macroscopic filtration law for transient linear viscoelastic fluid flow in porous media. *International Journal of Engineering Science*, 38(5):487–504, 2000.

[31] A. W. Liu, D. E. Bornside, R. C. Armstrong, and R. A. Brown. Viscoelastic flow of polymer solutions around a periodic, linear array of cylinders: comparisons of predictions for microstructure and flow fields. *Journal of Non-Newtonian Fluid Mechanics*, 77(3): 153–190, 1998.

[32] A. E. H. Love. *A treatise on the mathematical theory of elasticity*. Cambridge university press, 1927.

[33] M. J. Miles and A. Keller. Conformational relaxation time in polymer solutions by elongational flow experiments: 2. Preliminaries of further developments: chain retraction; identification of molecular weight fractions in a mixture. *Polymer*, 21(11):1295–1298, 1980.

[34] O. Mokhtari, Y. Davit, J.-C. Latché, and M. Quintard. A staggered projection scheme for viscoelastic flows. Working paper or preprint, 2021. URL `https://hal.archives-ouvertes.fr/hal-03400727`.

[35] O. Mokhtari, J.-C. Latché, M. Quintard, and Y. Davit. Birefringent strands drive the flow of viscoelastic fluids past obstacles. Submitted to Journal of Fluid Mechanics (under review: minor revisions), 2022.

[36] L. Molinet and R. Talhouk. Newtonian limit for weakly viscoelastic fluid flows of oldroyd type. *SIAM Journal on Mathematical Analysis*, 39(5):1577–1594, 2008.

[37] J. A. Odell and S. P. Carrington. Extensional flow oscillatory rheometry. *Journal of Non-Newtonian Fluid Mechanics*, 137(1-3):110–120, 2006.

[38] J. G. Oldroyd. On the formulation of rheological equations of state. *Proceedings of the Royal Society of London. Series A. Mathematical and Physical Sciences*, 200(1063): 523–541, 1950.

[39] R. G. Owens and T. N. Phillips. *Computational rheology*. World Scientific, 2002.

[40] J. M. Rallison and E. J. Hinch. Do we understand the physics in the constitutive equation? *Journal of Non-Newtonian Fluid Mechanics*, 29:37–55, 1988.

[41] Y. Saad and M. H. Schultz. GMRES: A generalized minimal residual algorithm for solving nonsymmetric linear systems. *SIAM Journal on Scientific and Statistical Computing*, 7(3):856–869, 1986.

[42] E. Sanchez-Palencia. On the asymptotics of the fluid flow past an array of fixed obstacles. *International Journal of Engineering Science*, 20(12):1291–1301, 1982.

[43] O. Scrivener, C. Berner, R. Cressely, R. Hocquart, R. Sellin, and N. S. Vlachos. Dynamical behaviour of drag-reducing polymer solutions. *Journal of Non-Newtonian Fluid Mechanics*, 5:475–495, 1979.

[44] D. O. Shah. *Improved oil recovery by surfactant and polymer flooding*. Elsevier, 2012.

[45] J. C. Slattery. Flow of viscoelastic fluids through porous media. *AIChE Journal*, 13(6): 1066–1071, 1967.

[46] M. M. Smith, J. A. K. Silva, J. Munakata-Marr, and J. E. McCray. Compatibility of polymers and chemical oxidants for enhanced groundwater remediation. *Environmental Science & Technology*, 42(24):9296–9301, 2008.

[47] K. S. Sorbie. *Polymer-improved oil recovery*. Springer Science & Business Media, 2013.

[48] A. Souvaliotis and A. N. Beris. Spectral collocation/domain decomposition method for viscoelastic flow simulations in model porous geometries. *Computer Methods in Applied Mechanics and Engineering*, 129(1-2):9–28, 1996.

[49] C.-l. Sun and H.-Y. Huang. Measurements of flow-induced birefringence in microfluidics. *Biomicrofluidics*, 10(1):011903, 2016.

[50] K. K. Talwar and B. Khomami. Application of higher order finite element methods to viscoelastic flow in porous media. *Journal of Rheology*, 36(7):1377–1416, 1992.

[51] M. Van Dyke. Perturbation methods in fluid mechanics. *NASA STI/Recon Technical Report A*, 75:46926, 1975.

[52] W. Voigt. *Lehrbuch der kristallphysik:(mit ausschluss der kristalloptik)*, volume 34. BG Teubner, 1910.

[53] K. Walters and M. F. Webster. The distinctive CFD challenges of computational rheology. *International Journal for Numerical Methods in Fluids*, 43(5):577–596, 2003.

[54] S. Whitaker. Flow in porous media I: A theoretical derivation of Darcy's law. *Transport in Porous Media*, 1(1):3–25, 1986.

[55] S. Whitaker. *The method of volume averaging*. Kluwer Academic Publishers, 1999.